MATCH Commun. Math. Comput. Chem. 95 (2026) 603-619

ISSN: 0340-6253

doi: 10.46793/match.95-3.05325

Experimental Realisation of Nut Graphs Using Coaxial Cable Networks

Maxine M. McCarthy^{a*†}, David M. Whittaker^a, Patrick W. Fowler^b, Barry T. Pickup^b

^a Physics and Astronomy, School of Mathematical and Physical Sciences, University of Sheffield, Sheffield S3 7RH, UK

^b Chemistry, School of Mathematical and Physical Sciences, University of Sheffield, Sheffield S3 7HF, UK

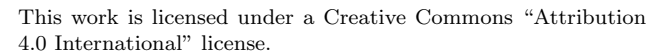
Maxine.McCarthy@mpl.mpg.de, D.M.Whittaker@sheffield.ac.uk, P.W.Fowler@sheffield.ac.uk, B.T.Pickup@sheffield.ac.uk

(Received Sunday 9th November, 2025)

Abstract

A nut graph is a connected simple graph with nullity one that has a full kernel eigenvector. In the context of π systems, chemical nut graphs are identical with the subcubic nut graphs. Chemical nut graphs are of interest for at least two reasons: the possibility of fully distributed radical reactivity arising from partial occupation of their sole non-bonding orbital, and their identification with the class of strong omniconductors of nullity one in source-and-sink models of ballistic molecular conduction. In this note, a mapping between the Hückel tight-binding theory of π -conjugated carbon frameworks and the Telegraph equations for networks of coaxial cables is described. This mapping motivates experimental realisation of chemical nut graphs, where the radio-frequency resonances of the cable network correspond to the spectrum of a weighted version of the molecular

 $^{^\}dagger \text{Present}$ address: Max Planck Institute for the Science of Light, Staudtstraße 2, 91058 Erlangen, Germany





^{*}Corresponding author

graph. In particular, measurements with a vector network analyser give direct access to the nullstate of the cable network, and hence to a simulation of the non-bonding molecular orbital of the π system. We demonstrate the distributed nature of the kernel eigenvector, which underpins the description of chemical reactivity, omni-conduction and electrical properties, for the cable models of the smallest chemical nut graph, and the three smallest nut graphs. We also show the feasibility of larger cable networks obtainable by known constructions for infinite families of nut graphs.

1 Introduction

The special properties of nut graphs have attracted attention in both mathematics and chemistry [11, 22–26]. A nut graph is a simple graph (unweighted, without loops or parallel edges) for which the 0,1 adjacency matrix has a single zero eigenvalue, and for which the kernel eigenvector has no zero entries. It is straightforward to show that nut graphs are connected, have no vertices of degree 1, and are non-bipartite [27]. Traditionally, the graph consisting of an isolated vertex is considered to be a trivial case [27]. Hence, the smallest non-trivial nut graphs have 7 vertices; these are the three Sciriha graphs shown in Fig. 1. As cycles have nullity either 0 or 2, every non-trivial nut graph has at least one vertex of degree > 2. Extensive catalogues of nut graphs of various classes have been compiled [1–3].

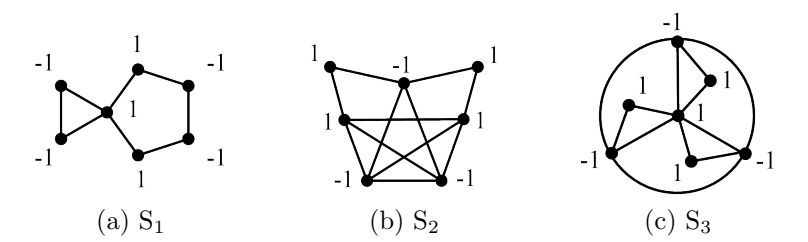


Figure 1. The Sciriha graphs: the three smallest nut graphs, with kernel eigenvectors.

In chemistry, the focus is on *chemical* nut graphs. Chemical graphs are intended to represent possible carbon skeletons of conjugated systems, and therefore they are defined here as connected simple graphs with maximum

degree ≤ 3 . The chemical nut graphs are then exactly the subcubic nut graphs. As a nut graph has no leaves, and is not a cycle, an n-vertex chemical nut graph has v_2 vertices of degree 2 and v_3 of degree 3, where $n = v_2 + v_3$, $v_2 \ge 0$, $v_3 > 0$, and v_3 is even. Chemical nut graphs exist for all pairs (v_2, v_3) satisfying these inequalities, apart from a finite set of pairs at small orders, and two specific infinite families with small v_3 : i.e. for pairs $(v_2, 2)$ with v_2 is even, and $(v_2, 4)$ with v_2 odd, there is no chemical nut graph [8]. Proof of these results for chemical nut graphs relied upon the existence of constructions by which nut graphs of higher order n can be produced from smaller nut graphs either by insertion of vertices on edges, or replacement of degree-3 vertices with a specific hexagonal motif. The smallest chemical nut graph has 9 vertices and is shown in Fig. 2 along with an 11-vertex chemical nut graph, constructed via insertion of two vertices on a cut edge (bridge) of the 9-vertex graph. Cubic polyhedral nut graphs $(v_2 = 0)$ include, for example, the Frucht graph [9] and some fullerenes [7, 26].

The defining feature of the nut graph is that the unique non-trivial kernel eigenvector (in chemical terms, the unique non-bonding π molecular orbital) is distributed over all vertices (conjugated carbon atoms). In some cases, the vector is equidistributive (has entries of equal magnitude on all vertices), but in general it may contain entries with different relative magnitudes. In any chemical nut graph, as there are at least two vertices of degree 3, the ratio of largest to smallest magnitudes of entries is at least 2:1 [3]. For example, the Sciriha graphs are all equidistributive, whereas the smallest chemical nut graph, Chem₁, is not, as it has one vertex entry that has twice the magnitude of the others (see Figures 1 and 2).

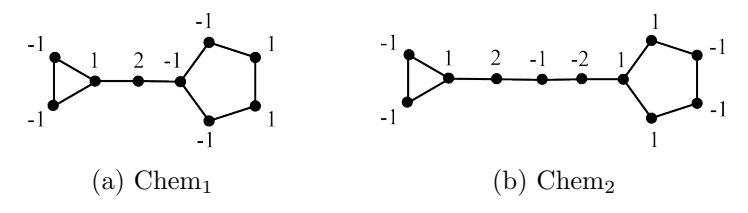


Figure 2. Kernel eigenvectors of chemical nut graphs: (a) Chem₁, the smallest chemical nut graph; (b) Chem₂, constructed by adding two vertices on the bridge of Chem₁.

Nut graphs are of interest in chemistry for two reasons that both stem from this distributed nature of the kernel eigenvector. The first concerns reactivity. If the zero eigenvalue in the spectrum of a chemical nut graph occurs at the HOMO-LUMO frontier for some accessible electron count, then the nature of the kernel eigenvector implies that, within the Hückel approximations, there will be a doublet state with non-zero spin density, and hence radical reactivity, on all carbon centres. The second reason concerns molecular conduction. In the Hückel version of the SSP model of ballistic conduction for two-wire devices [19], nut graphs are exactly the strong omniconductors of nullity 1, i.e. they have Fermi-level conduction for all distinct and ipso contact pairs, at least within the Hückel model [6], precisely because every vertex of a nut graph is a core vertex (carries non-zero density in the kernel eigenvector) [28].

In the present note, we consider an approach to nut graphs that is based on an analogy between Hückel theory (the simplest tight-binding theory) and the radio-frequency theory of coaxial cable networks. Specific states of the cable network correspond to the *non-bonding* orbitals of an analogous π system. This analogy allows realisation of a nut graph as a macroscopic object with measurable electrical properties that derive from the defining property of these graphs, and gives a strategy for making larger cable networks by straightforward use of the known mathematical constructions for nut graphs.

The structure of the paper is as follows. The connection between nut graphs and the source-and-sink model of ballistic molecular conduction is reprised in §2. The mathematical basis of the chemical graph/cable network analogy is set out in §3 and the experimental method and results are described in §4. Finally, some conclusions and perspectives are offered in §5.

2 Nut graphs and the SSP model

Nut graphs were originally defined with respect to their special role in graph theory. However, they also occupy a special position in the source-and-sink-potential (SSP) model [10] for ballistic conduction in molecular

devices. In the graph theoretical tight-binding formulation [20], incorporation of a molecular π system in a circuit is represented by attaching the molecular graph via single bonds to semi-infinite leads modelled as chains of atoms. If G is the molecular graph and the vertices of G that are in contact with the left and right leads (not necessarily distinct) are \bar{L} and \bar{R} , then the transmission of an incoming electron with zero energy is given by a simple function of four graph characteristic polynomials. The DC transmission at the zero of energy (the π non-bonding level) and in the wide-band limit, at all energies, is given by [20]

$$T_{\rm SSP}(0) = \frac{4(u_0 t_0 - s_0 v_0)\tilde{\beta}^2}{(s_0 - \tilde{\beta}^2 v_0)^2 + (u_0 + t_0)^2 \tilde{\beta}^2}$$
(1)

with s_0 , t_0 , u_0 , v_0 denoting characteristic polynomials, evaluated in the limit of zero energy, of the graphs G, $G - \bar{L}$, $G - \bar{R}$, and $G - \bar{L} - \bar{R}$, respectively. This expression can be used in conjunction with the Interlacing Theorem to derive selection rules for conduction/insulation at zero energy by considering the nullities of these four vertex-deleted graphs, *i.e.* the numbers of zero roots of the polynomials s(E), t(E), u(E), and v(E) [20]. In the case of nut graphs, which figure prominently in this paper, u_0t_0 is non-zero, whereas s_0v_0 is zero.

A useful distinction is between core and core-forbidden vertices [28]. A core vertex (CV) of a graph is one that has a non-zero entry in some vector in the kernel of the adjacency matrix of that graph. All vertices that are not core are core forbidden (CFV). Deletion of a core vertex reduces nullity by one; deletion of a core-forbidden vertex leaves nullity unchanged or increases it by one, a distinction recognised in the finer classification of CFV into middle (CFV_{middle}) and upper (CFV_{middle}) subtypes. By definition, all vertices of a nut graph are core vertices, and the expression ut-sv is therefore non-vanishing at zero energy for these graphs, implying $T(0) \neq 0$ for all pairwise connections of a nut graph, whether distinct or not. Hence, in the terminology developed for the SSP model [6], the nut graphs are strong omniconductors (in fact, they are exactly the strong omniconductors of nullity one).

The entries in the kernel eigenvector of a chemical nut graph are easily

assigned from the local condition that the sum of entries in the kernel vector over the neighbours of any vertex vanishes. The trick of assigning variables by pivoting on each vertex in turn, and using simple logic to eliminate redundant variables has a long history in chemistry [15]. As the nullity of a nut graph is one, all entries in the kernel eigenvector are multiples of a single parameter, enabling comparison at a glance with the cable network experiments described below.

3 Coaxial cable networks

Coaxial cables were patented by Heaviside in 1880 [17] as a means of allowing signal propagation with minimal interference from external electromagnetic influences. A coaxial cable consists of a pair of concentric cylindrical conductors, separated by a dielectric material. It is characterised by two parameters: the propagation speed, c, determined by the refractive index of the dielectric, and the impedance, Z, which depends on the ratio of the diameters of the two conductors. Signal propagation in such cables is described by Heaviside's Telegraph equations [12,14]. In the absence of losses, these reduce to simple one-dimensional wave equations for the voltage, V(x,t) and current I(x,t). These yield monochromatic solutions of the form $V(x,t) = V(x)e^{-i\omega t}$ with

$$V(x) = V(0)\cos(\omega x/c) + iZI(0)\sin(\omega x/c), \qquad (2)$$

where the current is $I(x) = (ic/\omega Z)dV/dx$. In a network, this implies that the voltages V_n and $V_{n'}$ on two vertices, connected by a cable with length $d_{nn'}$ and impedance $Z_{nn'}$, are related by

$$V_{n'} = V_n \cos(\omega d_{nn'}/c) + iZ_{nn'}I_{nn'} \sin(\omega d_{nn'}/c), \qquad (3)$$

where $I_{nn'}$ is the current flowing out of vertex n towards vertex n'.

In order to produce a network that maps onto a tight binding model, we choose the lengths of the cables such that the propagation time, $\tau = d/c$, is the same in each. In this work, we use identical cables, such that all have the same length and the same impedance, $Z_0 = 50\Omega$. Charge conservation

(Kirchhoff's First Law) requires the net current flowing out of a vertex to be zero, so

$$iZ_0 \sin \omega \tau \sum_{\langle n' \rangle} I_{nn'} = \sum_{\langle n' \rangle} (V_{n'} - V_n \cos \omega \tau) = 0 ,$$
 (4)

where $\langle n' \rangle$ indicates the set of neighbours that are connected to vertex n. This leads to a generalised eigenvalue problem

$$\sum_{\langle n' \rangle} V_{n'} = \sum_{\langle n' \rangle} \bar{H}_{nn'} V_{n'} = \varepsilon \deg(n) V_n , \qquad (5)$$

where \bar{H} is the adjacency matrix of the graph, $\varepsilon = \cos(\omega \tau)$ and $\deg(n)$ is the degree of vertex n. To obtain a tight-binding form, we scale the voltage at each vertex, defining $v_n = \sigma^{-1}V_n$, where $\sigma_n = (\deg(n))^{-1/2}$. Then Eq. (5) can be written as a standard eigenvalue problem

$$\sum_{\langle n'\rangle} H_{nn'} \, v_{n'} = \varepsilon \, v_n \,\,, \tag{6}$$

where $H_{nn'} = \sigma_n \bar{H}_{n,n'} \sigma_{n'}$. The cable network thus maps onto a weighted graph, and typically eigenvectors of H and \bar{H} do not coincide. There are two systematic exceptions. The first is for regular graphs, where all eigenvectors are in common, and eigenvalues of \bar{H} and H are related by a single scaling factor equal to the degree. The other is for singular graphs (graphs with a zero eigenvalue). In this latter case, any zero-energy state of the generalised problem, Eq. (5), is also an eigenstate with $\varepsilon = 0$ of the unweighted adjacency matrix, \bar{H} , and vice versa, implying equal nullity of the two graphs. Thus, in the experiments we will be able to measure the true nullstates of the nut-graph. Note that the eigenvalue, ε , is a dimensionless quantity, but we will nevertheless describe it as an 'energy', by analogy with the language of tight-binding theory. The zero of this energy corresponds to a finite frequency, $\omega \tau = \pi/2$.

When driven with a radio-frequency source, using a vector network analyser (VNA), the cable network will have resonances at frequencies, ω , corresponding to the eigenvalues $\varepsilon_k = \cos \omega \tau$ of Eq. (6). This provides an

experimental measurement of the spectrum of the weighted graph. Specifically, as shown in Ref. 29, the impedance of the network measured at connection vertex α is

$$Z_{\alpha}(\varepsilon) = iZ_0 \sqrt{1 - \varepsilon^2} \sum_{k} \frac{|V_{\alpha}^{(k)}|^2}{\varepsilon_k - \varepsilon} , \qquad (7)$$

where $V_{\alpha}^{(k)}$ is the amplitude of the k^{th} eigenvector of Eq. (5) on the vertex. Apart from a trivial factor, the real part of $Z_{\alpha}(\varepsilon)$ at the pole is the local density of states at the vertex α . The impedance plot for a vertex therefore consists of a series of delta function peaks, *i.e.* resonances, at the eigenvalues for which the density of states at that vertex is non-zero. In practice, these resonances are broadened slightly by losses in the cables, which may lead to residual signal, even where the density of states at the vertex is nominally zero. The intensity of a peak is essentially $|V_{\alpha}^{(k)}|^2$, and so measuring impedance at all the vertices in the network allows us to plot the spatial structure of a given eigenvector, and in particular to identify the core and core-forbidden vertices of the graph. These are easily distinguished, as the measurements give access to response across the whole frequency range.

We also measure amplitude and phase of the complex transmission for any chosen pair of vertices. This allows us to demonstrate, for example, the strong omniconducting behaviour of the graph S_3 , and also, at least in the case of graphs with nullity 1, to determine the relative signs of the entries in the nullstate vector on different core vertices.

When, as here, we have a non-degenerate state at $\varepsilon=0$, the transmission depends on the amplitudes of this state, on the input vertex α and the output vertex β . This allows us to use the sign of the transmission amplitude at $\varepsilon=0$ to measure the relationship between the signs of $V_{\alpha}^{(0)}$ and $V_{\beta}^{(0)}$. The situation is complicated by the effects of the losses due to the finite input and output impedances of the VNA, equivalent to source and sink dissipation in the SSP model. Taking these into account, we find the transmission amplitude, $t_{\beta\alpha}(\varepsilon)$, at zero energy for our case of interest,

the nut graph, to be

$$t_{\beta\alpha}(0) = \frac{iV_{\beta}^{(0)}V_{\alpha}^{(0)}}{-\sum_{\varepsilon_{k}\neq 0} \varepsilon_{k}^{-1} \left(V_{\alpha}^{(k)}V_{\beta}^{(0)} - V_{\beta}^{(k)}V_{\alpha}^{(0)}\right)^{2} + i\left((V_{\alpha}^{(0)})^{2} + (V_{\beta}^{(0)})^{2}\right)},$$
(8)

where the sum in the first term in the denominator is over all the non-zero eigenstates of Eq. (5), with energies ε_k and amplitudes $V_{\alpha}^{(k)}$ and $V_{\beta}^{(k)}$ on the input and output vertices. These loss terms lead to a non-zero phase for $t_{\beta,\alpha}(\varepsilon=0)$. However, as the imaginary part of the denominator in Eq. (8) is greater than zero, the real part $\text{Re}\{t_{\beta\alpha}\}$ is a product of a positive quantity and $V_{\beta}^{(0)}V_{\alpha}^{(0)}$. Using this fact, the relative signs of the nullstate entries on each vertex can be measured experimentally, providing a full tomography of the state, and effectively a proxy for measurement of the non-bonding π molecular orbital.

The quantity $|t_{\beta,\alpha}(\varepsilon=0)|^2$ derived from Eq. (8) is not equal to the Fermi level transmission for the molecular graph in the SSP model, $T_{\rm SSP}$, but zero/non-zero values of the two quantities are matched, as this depends on vanishing/non-vanishing of products of entries in the nullstate/non-bonding orbital vector. In the molecular-orbital/channel formulation of the SSP model [21], Fermi-level transmission through a nut graph takes the same form as the expression for $|t_{\beta,\alpha}(\varepsilon=0)|^2$ derived from Eq. (8). (Take Case 9 and 10 of Table I in [21], set all Hückel resonance integrals to unity, and use Laurent expansions of numerator and denominator.) Where the expressions for $|t_{\beta,\alpha}(\varepsilon=0)|^2$ and $T_{\rm SSP}(0)$ differ, however, is that the denominator of $|t_{\beta,\alpha}(\varepsilon=0)|^2$ involves eigenvalues of H, i.e. ε_k , whereas the denominator of $T(0)_{\rm SSP}$ involves eigenvalues of the unweighted adjacency matrix of \bar{H} .

The transmission (Eq. (8)) is specific to the case of nullity 1. For $\eta > 1$, the numerator of Eq. (8) becomes a sum involving a shell invariant that depends on the two vertices α and β , so that sign information for the specific basis vectors cannot be recovered immediately from the transmission in the same way as when nullity is 1.

4 Experiments

We have carried out an experimental investigation of the null states of the various nut graphs discussed above, using radio frequency measurements on the coaxial cable networks that represent them. We use type RG58 cables which have an impedance of 50 Ω . The lengths of the cables are approximately 41 cm, and hence the condition for zero energy ($\omega \tau = \pi/2$) corresponds to a frequency around 114 MHz. Each cable is made with an SMA female connector at one end and a male connector at the other. They can therefore be joined directly to form a vertex of degree two, whilst a standard T-connector provides degree three. This is exactly what is required to represent chemical graphs, but for degrees greater than three, it is necessary to stack multiple T-connectors to make the junction. Fig. 3 shows photographs of experimental cable networks for several nut graphs.



Figure 3. Photographs of physical cable networks that simulate nut graphs S_1 , S_2 , and S_3 . Edges (cables) are labelled in white, vertices (connectors) are bronze-coloured, and the respective degree sequences are 2^64^1 , 2^24^5 , $2^34^36^1$.

We make two sorts of radio frequency measurement with a VNA: the impedance obtained at each vertex gives the amplitude of the state, and transmission measurements provide the information required to determine the relative signs. Typical experimental data are shown in Fig. 4(a), for a network corresponding to the Sciriha graph S1. In the impedance spectra, the states appear as narrow peaks, broadened by the resistive losses in the cables. By integrating over the region of the peak and comparing with Eq. (7), we obtain $|V_n|^2$, the squared amplitude on vertex n. This measurement for each vertex in the network allows us to perform a tomography of the state by combining it with transmission measurements: the relative sign of the amplitudes on a pair of vertices is given by the sign of

the real part of the transmission at $\varepsilon = 0$, see Eq. (8). By choosing an input vertex, and measuring the transmission to all the other vertices, we can determine the relative signs of the state on each vertex. This enables us to plot the nullstate, as in Fig. 4(b), where the radius of each circle is proportional to the amplitude of the state on that vertex, and the colour indicates the sign.

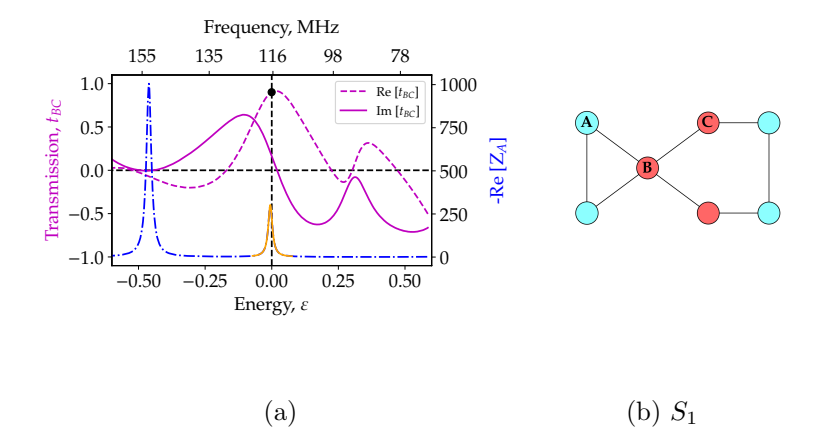


Figure 4. (a) Examples of experimental measurements of the real part of the impedance, $\operatorname{Re}[Z_A]$ (RH scale, blue dot-dashed curve) and transmission, t_{BC} (LH scale, real/ imaginary components magenta solid/dashed curves). The measurements were made on cable network (b), representing Sciriha graph S_1 , recording impedance at vertex \mathbf{A} , and transmission between \mathbf{B} and \mathbf{C} . Similar measurements were used to obtain the amplitude of the nullstate on each vertex of the graph: the modulus is found by integrating the impedance over the window $-0.08 < \varepsilon < 0.08$ (orange) and using Eq.(7) to obtain $|V_n|^2$. Relative signs are deduced from transmission between pairs of sites (see Eq. (8) and discussion). The radius of each vertex in (b) is proportional to experimental amplitude, V_n , with colour indicating sign. Measured and theoretical nullstates agree, with fidelity 99.9%.

In Fig. 5 we show the experimental nullstates for the networks representing the two remaining 7-vertex nut graphs, S_2 and S_3 . Fig. 6 shows the results for the smallest chemical nut graph, and the chemical nut graph constructed by the addition of two vertices to the bridge, demonstrating experimentally that this construction indeed creates a new nut graph.



Figure 5. Experimentally determined nullstates for cable networks representing Sciriha graphs S_2 and S_3 , using the method illustrated in Fig. 4. The radius of each vertex is proportional to the amplitude, V_n , and colours indicate relative signs. In both, fidelity between theory and experiment is 99.2%.



Figure 6. Experimental nullstates for networks representing (a) the smallest chemical nut graph, and (b) a chemical nut graph constructed with the addition of two vertices on a bridge. The amplitude of the state is proportional to the radius of the vertex, and colour indicates the sign. The fidelity is 98.6% for (a) and 99.8% for (b).

As a measure of how well the experiments reproduce the theoretical nullstate, we calculate the *fidelity* of the experimental measurement, defined by

$$F = |V^{\text{graph}^T} V^{\text{exp}}|^2, \tag{9}$$

where $V^{\rm graph}$ is the theoretical kernel eigenvector, and $V^{\rm exp}$ is the experimental nullstate, both being normalised to unity. All our measurements give fidelities between 98.6% and 99.9%, demonstrating excellent agreement with theory.

In Fig. 7 we present experimental data confirming the *strong* omniconduction of the graph S_3 . Two sets of measurements were taken. Transmission for vertex pairs demonstrates the distinct omniconduction, whilst

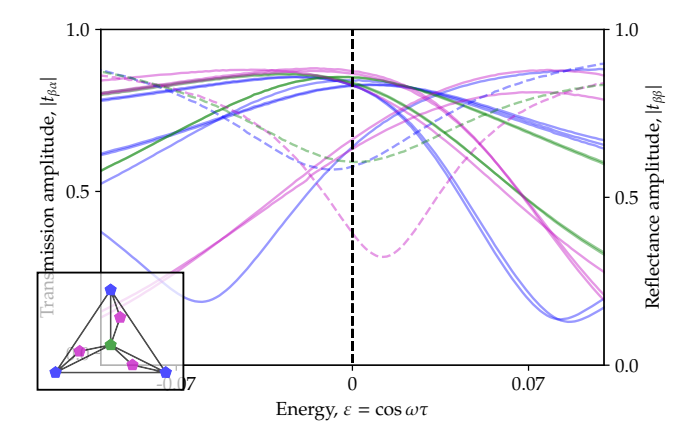


Figure 7. Experimental demonstration of strong omniconduction for nut graph S_3 (inset). The symmetry of the graph implies that full demonstration requires only transmission measurements between one vertex of each orbit (blue, green, magenta) and all other vertices of the graph. Absolute values of the transmission are plotted (solid curves, coloured by input vertex). The transmission at $\varepsilon=0$ is always non-zero, confirming distinct omniconduction. Also shown (dashed) is the absolute value of the reflectance spectrum for one vertex of each orbit, demonstrating ipso-omniconduction.

reflectance, measured for one vertex at a time, demonstrates the ipso-omniconduction. We plot the absolute value of the transmission, $|t_{\beta\alpha}|$. In all cases, $|t_{\beta\alpha}|$ at $\varepsilon=0$ is much greater than zero, demonstrating distinct omniconduction. The figure also shows the absolute reflectance at each input. This too is non-zero at $\varepsilon=0$, and hence ipso-omniconduction is also apparent.

5 Conclusions

This work on a crossover between graph theory/mathematical chemistry and experimental physics follows in a tradition of using macroscopic models to illustrate concepts and supply scaffolding for future investigations. Past examples from theoretical chemistry/ chemical physics and from the theory of electromagnetism include use of electrical circuit analogues for the secu-

lar determinants in the theory of molecular vibrations [30], and, famously, Maxwell's initial mechanical model of the electromagnetic field [13,16,18]. The present approach gives a visualisation of a (one-electron) wavefunction captured via a physical model embodied in a macroscopic cable network.

The nut graphs investigated here happen to have mixed vertex degree. However, nut graphs can also be regular. In particular, cubic nut graphs exist for n=12 and all even $n\geq 18$ [8], and these can be partitioned into uniform, balanced or unbalanced classes, according to the pattern of entries in the kernel eigenvector [26]. Cubic nut graphs include some classics of graph theory, such as the Frucht graph. The tripartite uniform/balanced/unbalanced classification would be amenable to investigation using one-port measurements.

Another obvious extension would be to *core graphs* (graphs where all vertices are core vertices, but nullity may exceed one), for which the cable network invariants will correspond to partial spin/charge densities resulting from occupation of the nullspace of a π system.

Directions for further exploration of the analogy with the SSP model include systematic simulation of the selection rules for ballistic conduction at E=0 of distinct (11 cases) and ipso (3 cases) devices, which are based on the nullity signature of the polynomials s,t,u,v and of the combination $j^2=ut-sv$. Every case can be found in some chemical graph. Note that the commonality of kernels of weighted and unweighted graphs extends to the related vertex-deleted graphs, implying that the vertices of weighted and unweighted graphs have identical partitions into types CV, CFV_{middle}, CFV_{upper}, whatever the value of η . It follows from this that the conduction cases derived for E=0 from weighted and unweighted graphs are the same.

It could also be interesting to work with the TLA (three-letter-acronym) classification of molecular graphs, both bipartite and non-bipartite, and sets of devices that can be derived from them [4]. Exotica such as the Clar Goblet, a concealed non-Kekulean benzenoid, could also be of interest.

Beyond the realm of graphs, an interesting extension would be to digraphs with specific properties of their kernels and cokernels. Cable networks that mimic directed graphs are realisable with standard components, and research on this is being pursued in Sheffield. Acknowledgment: The authors thank the International Centre for Mathematical Sciences for support in connection with the International Workshop on Optimal Network Topologies (IWONT2023). DMW and MMM thank EPSRC for a PhD studentship to MMM. PWF thanks the Leverhulme Trust for an Emeritus Fellowship on 'Modelling molecular currents, conduction and aromaticity'.

References

- [1] G. Brinkmann, K. Coolsaet, J. Goedgebeur, H. Mélot, House of Graphs: a database of interesting graphs, *Discr. Appl. Math.* **161** (2013) 311–314.
- [2] K. Coolsaet, P. W. Fowler, J. Goedgebeur, Nut graphs, homepage of Nutgen, http://caagt.ugent.be/nutgen/.
- [3] K. Coolsaet, P. W. Fowler, J. Goedgebeur, Generation and properties of nut graphs, MATCH Commun. Math. Comput. Chem. 80 (2018) 423–444.
- [4] P. W. Fowler, M. Borg, B. T. Pickup, I. Sciriha. Molecular graphs and molecular conduction: the d-omni-conductors, *Phys. Chem. Chem. Phys.* 22 (2020) 1349–1358.
- [5] P. W. Fowler, J. B. Gauci, J. Goedgebeur, T. Pisanski, I. Sciriha, Existence of regular nut graphs for degree at most 11, *Discuss. Math. Graph Theory* 40 (2020) 533–557.
- [6] P. W. Fowler, B. T. Pickup, T. Z. Todorova, M. Borg, I. Sciriha, Omni-conducting and omni-insulating molecules, J. Chem. Phys. 140 (2014) #054115.
- [7] P. W. Fowler, B. T. Pickup, T. Z. Todorova, R. De Los Reyes, I. Sciriha, Omni-conducting fullerenes, *Chem. Phys. Lett.* 568–569 (2013) 33–35.
- [8] P. W. Fowler, T. Pisanski, N. Bašić, Charting the space of chemical nut graphs, MATCH Commun. Math. Comput. Chem. 86 (2021) 519– 538.
- [9] J. B. Gauci, T. Pisanski, I. Sciriha, Existence of regular nut graphs and the Fowler construction, *Appl. Anal. Discr. Math.* (2020), in press. (See https://arxiv.org/abs/1904.02229)

- [10] F. Goyer, M. Ernzerhof, M. Zhuang, Source and sink potentials for the description of open systems with a stationary current passing through, J. Chem. Phys. 126 (2007) #144104.
- [11] I. Gutman, I. Sciriha, Graphs with maximum singularity, Graph Theory Notes N. Y. 30 (1996) 17–20.
- [12] O. Heaviside, XIX. On the extra current, Lond. Edinb. Dublin Phil. Mag. J. Sci., 2 (1876) 135–145.
- [13] B. J. Hunt, Maxwell, measurement, and the modes of electromagnetic theory, *Hist. Stud. Nat. Sci.* **45** (2015) 303–339.
- [14] B. J. Hunt, *The Maxwellians*, Cornell Univ. Press, Ithaca, 2005, pp. 66–67.
- [15] H. C. Longuet-Higgins, Some studies in molecular orbital theory I. Resonance structures and molecular orbitals in unsaturated hydrocarbons, J. Chem. Phys. 18 (1950) 265–274.
- [16] B. Mahon, The Man Who Changed Everything: The Life of James Clerk Maxwell, Wiley, Chichester, 2004. (See Chapter 7: Spinning cells.)
- [17] K. D. Mayne, Heaviside's communication cable designs, *Electronics and Power* 23 (1977) 710–711.
- [18] J. C. Maxwell, XLIV. On physical lines of force, Part II The theory of molecular vortices applied to electric currents, Lond. Edinb. Dublin Phil. Mag. J. Sci. 21 (1861) 281–291.
- [19] B. T. Pickup, P. W. Fowler, An analytical model for steady-state currents in conjugated systems, *Chem. Phys. Lett.* 459 (2008) 198– 202.
- [20] B. T. Pickup, P. W. Fowler, A selection rule for molecular conduction, J. Chem. Phys. 131 (2009) #044104.
- [21] B. T. Pickup, P. W. Fowler, M. Borg, I. Sciriha, A new approach to the method of source-sink potentials for molecular conduction, J. Chem. Phys. 143 (2015) #194105.
- [22] I. Sciriha, On the construction of graphs of nullity one, *Discr. Math.* **181** (1998) 193–211.
- [23] I. Sciriha, On the rank of graphs, in: Y. Alavi, D. R. Lick, A. Schwenk (eds.), Combinatorics, Graph Theory, and Algorithms, Volume II, New Issues Press, Kalamazoo, 1999 pp. 769–778.

- [24] I. Sciriha, A characterization of singular graphs, El. J. Lin. Algebra 16 (2007) 451–462.
- [25] I. Sciriha, Coalesced and embedded nut graphs in singular graphs, Ars Math. Contemp. 1 (2008) 20–31.
- [26] I. Sciriha, P. W. Fowler, Nonbonding orbitals in fullerenes: nuts and cores in singular polyhedral graphs, J. Chem. Inf. Model. 47 (2007) 1763–1775.
- [27] I. Sciriha, I. Gutman, Nut graphs: maximally extending cores, Util. Math. 54 (1998) 257–272.
- [28] I. Sciriha, X. Mifsud, J. L. Borg, Nullspace vertex partition in graphs, J. Comb. Opt. 42 (2021) 310–326.
- [29] D. M. Whittaker, M. M. McCarthy, Q. Duan, Observation of a topological phase transition in random coaxial cable structures with chiral symmetry, arXiv:2311.11040 (2023), doi: https://doi.org/10.48550/arXiv.2311.11040.
- [30] E. B. Wilson, J. C. Decius, P. C. Cross, *Molecular Vibrations*, Dover Pub., New York, 1980. (see Chapter 9.)